

PROPERTIES OF $e\mu$ EVENTS PRODUCED IN $e^+ - e^-$ ANNIHILATION*†

Martin L. Perl

Stanford Linear Accelerator Center
Stanford University, Stanford, California 94301

TABLE OF CONTENTS

1. Introduction and Hypotheses	2
2. Experimental Method and Data	5
3. Summary of Background Studies	11
4. Evidence Using Improved Muon Detection	17
5. General Properties and Observed Cross Section	20
6. Angular Distributions	23
7. Momentum Distributions	29
8. Discussion and Conclusions	29
9. Acknowledgements	38

*Work supported by the U.S. Energy Research and Development Administration.

†This talk presented at the 1975 Topical Conference of the SLAC Summer Institute on Particle Physics has been revised to include information available up to October 1, 1975.

1. INTRODUCTION AND HYPOTHESES

The purpose of this talk is to describe the properties of the $e\mu$ events^{1,2} found in the data of the SLAC-LBL magnetic detector collaboration¹ using the SPEAR electron-positron colliding beams facility. The basic evidence for the $e\mu$ events will be summarized here (Sec. 3), but not fully discussed. New evidence using improved muon-pion separation will also be presented (Sec. 4). Most of the talk is devoted to the properties of the events, and the relations of those properties to various hypotheses as to the nature of the events. However this brief presentation of the evidence should not be taken to mean that we regard the evidence as no longer open to examination. We welcome critical examination of the evidence and the suggestion of alternative explanations of the events.

The $e\mu$ events have the form

$$e^+ + e^- \rightarrow e^+ + \mu^+ + \text{2-or-more undetected particles} \quad (1.1)$$

The undetected particles are charged particles or photons which escape 2.6π sr solid angle of the detector, or particles very difficult to detect such as neutrons, K_L^0 mesons, or neutrinos. In discussing hypotheses which may explain the $e\mu$ events I shall limit myself to the cases in which the events are the decay products of a pair of particles produced in the reaction

$$e^+ + e^- \rightarrow U^+ + U^- \quad (1.2)$$

The name U refers to the unknown nature of the particle. When the nature of the U particle is elucidated, assuming the pair production hypothesis is correct, a systematic or mnemonic name may be chosen. Hypotheses other than pair production were noted in Refs. 1 and 2, but we have not made any progress in developing such hypothesis. Perhaps we are being

short-sighted in this regard.

Next we consider some possibilities as to the nature of the U particle:

A. Heavy Leptons

Suppose the electron (e^\pm) and muon (μ^\pm) are the lowest mass members of a sequence of leptons,³⁻⁵ each lepton (ℓ^\pm) having a unique quantum number n_ℓ and a unique associated associated neutrino (ν_ℓ). Such sequential³ heavy leptons have the purely leptonic decay modes:

$$\ell^- \rightarrow \nu_\ell + e^- + \bar{\nu}_e, \ell^- \rightarrow \nu_\ell + \mu^- + \bar{\nu}_\mu \quad (1.3)$$

assuming the quantum number n_ℓ must be conserved as are n_μ and n_e . (The ℓ^+ has corresponding decay modes.) If the ℓ has a sufficiently large mass it will also have semileptonic decay modes.

$$\ell^- \rightarrow \nu_\ell + \pi^-, \ell^- \rightarrow \nu_\ell + K^-, \ell^- \rightarrow \nu_\ell + \rho^-, \ell^- \rightarrow \nu_\ell + 2 \text{ or more hadrons} \quad (1.4)$$

Other properties of the ℓ still have to be specified. The $\ell - \nu_\ell$ weak current may be V - A as with conventional leptons or it may be some other combination $\alpha V + \beta A$ where α and β are arbitrary.^{6,7} However with our present statistics we are content to use the V - A assumption for most of our illustrations. In addition the ν_ℓ might have a non-zero mass -- but again for simplicity we shall assume

$$\text{mass of } \nu_\ell = 0 \quad (1.5)$$

Finally we assume the ℓ has spin 1/2 leading to the pair production differential cross section

$$d\sigma_{ee \rightarrow \ell\ell}/d\Omega = \frac{\alpha^2 \beta}{4s} \left[(1 + \cos^2 \theta) + (1 - \beta^2) \sin^2 \theta \right] \quad (1.6)$$

in the laboratory frame. θ, ϕ are the angles of the ℓ^\pm ; the e^+e^- beams are assumed to be unpolarized; $\beta = v_\ell/c$ where v_ℓ is the velocity of the ℓ

in the laboratory frame; and the total energy is

$$\sqrt{s} = E_{\text{cm}} \quad (\text{also called } W) \quad (1.7)$$

Integrating over all angles:

$$\sigma_{ee \rightarrow \ell\ell} = \frac{43.4\beta(3 - \beta^2)}{E_{\text{cm}}^2} \text{ nb} \quad (1.8)$$

where E_{cm} is in GeV.

B. Heavy Mesons

If new charged mesons (M^\pm) exist which have relatively large leptonic decay modes (due to the inhibition of purely hadronic decay modes) then the purely leptonic decay modes.

$$M^- \rightarrow e^- + \bar{\nu}_e, \quad M^- \rightarrow \mu^- + \bar{\nu}_\mu; \quad (1.9)$$

can lead to the reaction in Eq. 1.1. Such charged mesons are predicted by theories which introduce the charmed quark.^{8,9} Of course, in an experimental search we need not restrict the interpretation of Eq. 1.9 to a particular theory -- indeed we shall not a priori restrict the mass or spin of M in this discussion. The M might also have semileptonic decay modes.

$$M^- \rightarrow e^- + \bar{\nu}_e + \text{hadrons}, \quad M^- \rightarrow \mu^- + \bar{\nu}_\mu + \text{hadrons} \quad (1.10)$$

The pair production cross section for the M is not known a priori.

I shall use a form

$$\sigma_{ee \rightarrow MM} = \frac{\eta \beta^3}{s} |F_M(s)|^2 \quad (1.11)$$

where η is a constant, $\beta = v_M/c$, β^3 is a guess at a threshold factor, and $F_M(s)$ is a production form factor.

C. New Baryons

The U might be a new type of baryon with decay modes such as

$$B^- \rightarrow e^- + \bar{\nu}_e + n, \quad B^- \rightarrow \mu^- + \bar{\nu}_\mu + n \quad (1.12)$$

where n is the neutron. Such baryons are predicted by the charmed hadron theories, and interestingly by an old speculation of M. Goldhaber¹⁰ on the doubling of fermions.

D. Elementary Bosons

Although the mass¹¹ of the intermediate bosons which is supposed to mediate the weak interaction (W^\pm), if it exists, is probably too high to allow pair production at the energies discussed in this paper; the decay modes

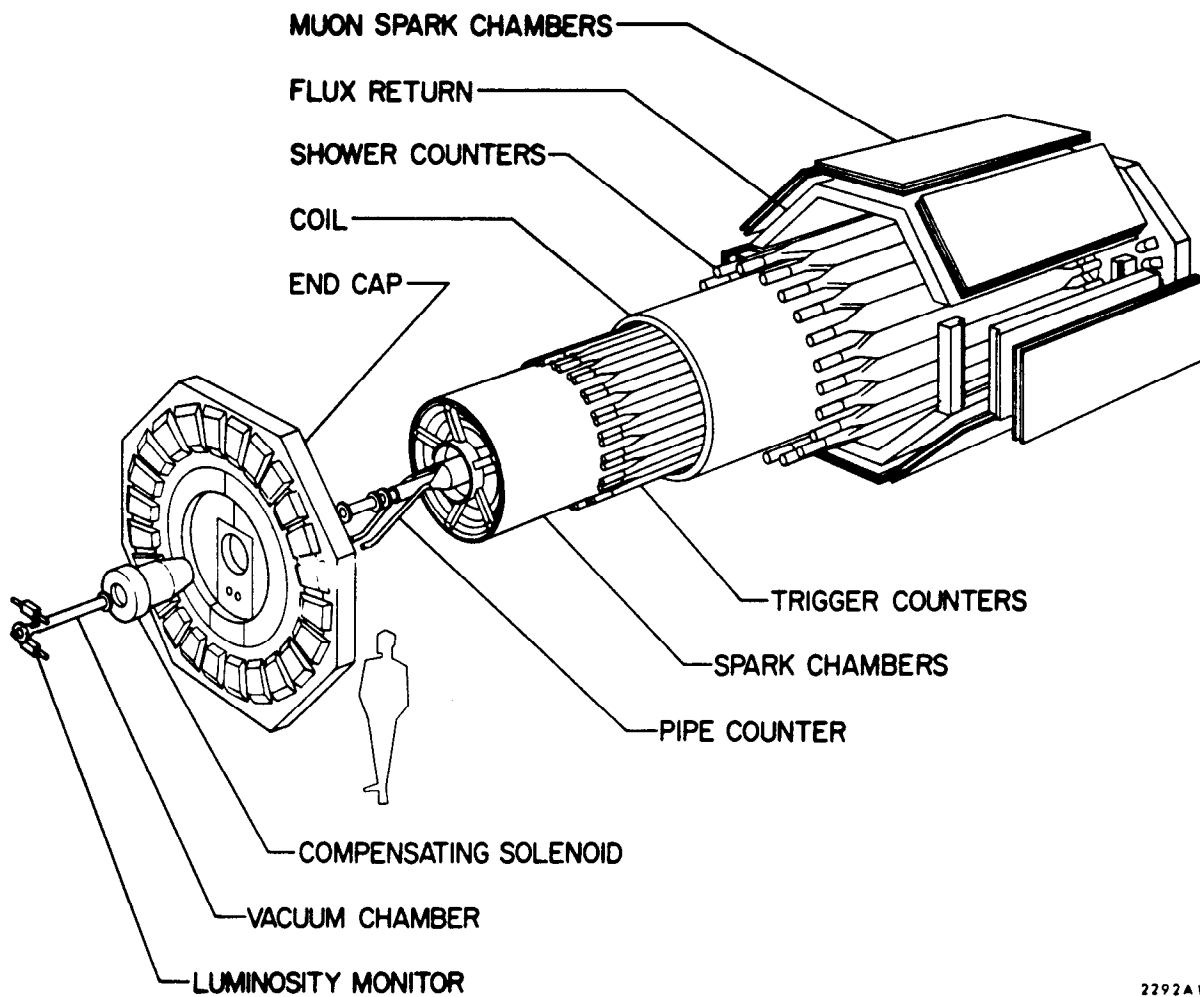
$$W^- \rightarrow e^- + \bar{\nu}_e, \quad W^- \rightarrow \mu^- + \bar{\nu}_\mu; \quad (1.13)$$

can lead to the reaction of Eq. 1.1

We may also consider other types of elementary bosons -- not necessarily the intermediate boson W. The difference between an elementary boson and a heavy meson is that we suppose the former to be a point particle with a form factor always equal to unity.

2. EXPERIMENTAL METHOD AND DATA

The magnetic detector^{12,13} (Fig. 1) used in the experiment has a 4 kg magnetic field produced by a coil of radius 1.65 m and length 3.6 m. Most of the space inside the coil, namely the magnetic field region, is occupied by cylindrical magnetostrictive spark chambers. The azimuthal angle, θ , subtended by these chambers extends from 50° to 130° relative to the e^+ beam direction. The full cylindrical angle of 2π is covered. Just inside the coil are 48, 2.6 m long, scintillation counters, and just outside the coil are 24, 3.1 m long, lead plastic-scintillator



2292A1

Fig. 1 The magnetic detector.

shower counters. The scintillation and shower counters cover the full 2π cylindrical angle. Outside the shower counters is the iron flux return which is 20 cm thick. Finally on the outside are magnetostrictive spark chambers called muon detection chambers. For particles to reach these chambers they must pass through the aluminum coil, the shower counters, the iron flux return and other material totaling 1.67 absorption lengths for pions. For the data acquired before January 1975, the entire lateral area of the detector was covered with muon detection chambers. After January 1975, 70% of the lateral area was so covered.

Electrons are identified solely by requiring a shower counter pulse height greater than that produced by a 0.5 GeV electron. Muon are identified by two requirements: the μ must be detected in one of the muon chambers and the shower counter pulse of the μ must be small. All other charged particles are called hadrons. The shower counters also detect photons (γ). For γ energies above 200 MeV, the γ detection efficiency is about 95%.

To find the $e\mu$ events of Eq. 1.1 we define a coplanarity angle

$$\cos \theta_{\text{copl}} = -(\underline{n}_1 \times \underline{n}_{e^+}) \cdot (\underline{n}_2 \times \underline{n}_{e^+}) / (|\underline{n}_1 \times \underline{n}_{e^+}| |\underline{n}_2 \times \underline{n}_{e^+}|) \quad (2.1)$$

where \underline{n}_1 , \underline{n}_2 , \underline{n}_{e^+} are unit vectors along the directions of particles 1, 2, and the e^+ beam. The contamination of events from the reactions $e^+e^- \rightarrow e^+e^-$ and $e^+e^- \rightarrow \mu^+\mu^-$ is greatly reduced if we require $\theta_{\text{copl}} > 20^\circ$.

To reach the muon chambers, Fig. 1, a particle must have a momentum greater than about 0.55 GeV/c. Therefore muons can only be identified at higher momenta. Also electrons of momentum below 0.5 GeV/c will be misidentified as pions more than half the time. Therefore to select $e\mu$ events we require that the momenta of particle 1 (p_1) and of particle 2 (p_2) each

be greater than 0.65 GeV/c. Thus the primary selection criteria for finding the $e\mu$ events are

- (1) 2-prongs
 - (2) $\theta_{\text{cop1}} > 20^\circ$
 - (3) $p_1 > 0.65$ GeV/c and $p_2 > 0.65$ GeV/c.
- (2.2)

The relative size of the event sample which meets the criteria in Eq. 2.2 compared to the numbers of other types of events is shown in Table I. Two examples are given, one involving a large statistics run at $E_{\text{cm}} = 4.8$ GeV and the other a set of runs in the energy interval $5.6 \leq E_{\text{cm}} \leq 6.8$ GeV

TABLE I

E_{cm} (GeV)	4.8	5.6 to 6.8
Number of 3-or-more prong events	9550	10,929
Number of $\theta_{\text{cop1}} < 20^\circ$ 2-prong events (mostly $ee \rightarrow ee$ and $ee \rightarrow \mu\mu$)	25,300	30,292
Number of $\theta_{\text{cop1}} > 20^\circ$ 2-prong events	2493	3237
Number of $\theta_{\text{cop1}} > 20^\circ$ $p_1 > 0.65$ GeV/c $p_2 > 0.65$ GeV/c 2-prong events	513	524

A tabulation of the types of events which meet the criteria of Eq. 2.2 is given in Tables IIa and IIb. In the tables the events are classified according to

- (1) Total charge (Q) : 0, \pm 2
- (2) Number of photons associated with event : 0, 1, or > 1 .

- (3) The charged particle nature e, μ , or h (for hadron). Any particle not an e or a μ is called an h.

We make the following observations on Table IIa and IIb

- (1) There are very few $Q = \pm 2$ events and we focus our attention on the $Q = 0$ events.
- (2) If there were no particle misidentification, no decays in flight, and no anomalous events we should see only
- (a) $e^+ e^-$ events from $e^+ + e^- \rightarrow e^+ + e^- + \gamma$, $e^+ + e^- \rightarrow e^+ + e^- + 2\gamma$, or from¹⁴ $e^+ + e^- \rightarrow e^+ + e^- + \mu^+ + \mu^-$.
- (b) $\mu^+ \mu^-$ events from similar reactions.
- (c) hh events.
- (3) The 24 or 17 $e\mu$ events in column 1 of Table IIa or IIb catch our attention immediately. We shall refer to them as the signature $e\mu$ events. If they cannot be explained by particle misidentification or decays in flight they constitute the anomalous leptonic signal of the reaction in Eq. 1.1. Incidentally they cannot come from the two-virtual-photon process,¹⁴

$$e^+ + e^- \rightarrow e^+ + e^- + \mu^+ + \mu^- \quad (2.3)$$

since we should see equal numbers of $e^+ \mu^+$ or $e^- \mu^-$; and we see only 0 or 1 such events (column 4 in Table IIa or IIb)

TABLE IIa

Distribution of 2-prong events, obtained at $E_{cm} = 4.8$ GeV, which meet the criteria: $|p_1| > 0.65$ GeV/c, $|p_2| > 0.65$ GeV/c, $\theta_{copl} > 20^\circ$.

Number Photons =	Total Charge = 0			Total Charge = ± 2		
	0	1	> 1	0	1	> 1
ee	40	111	55	0	1	0
e μ	24	8	8	0	0	3
$\mu\mu$	16	15	6	0	0	0
eh	20	21	32	2	3	3
μh	17	14	31	4	0	5
hh	14	10	30	10	4	6

TABLE IIb

Distribution of 2-prong events, obtained in the range $5.6 \leq E_{cm} < 6.8$ GeV, which meet the criteria $|p_1| > 0.65$ GeV/c, $|p_2| > 0.65$ GeV/c, $\theta_{copl} > 20^\circ$. There was only 70% muon chamber coverage for this data. Events in which neither prong points toward a muon chamber are not included; and non-e μ events in which only one prong points toward a muon chamber are counted as 0.5 events.

Number Photons =	Total Charge = 0			Total Charge = ± 2		
	0	1	> 1	0	1	> 1
ee	21	60	33.5	0	1	0
e μ	17	7	3	1	1	0
$\mu\mu$	13	9	6	1	0	1
eh	17	20.5	22	2	3.5	2
μh	13.5	14	21	0	0.5	3
hh	15	17	33.5	7.5	4.5	8

3. SUMMARY OF BACKGROUND STUDIES

The dominant contamination in the $e\mu$ events is from hadronic events in which two charged particles and no photons are detected; and (1) the detected hadrons are misidentified as an e or μ ; or (2) the detected charged particles are e 's or μ 's from hadron decays. Examples of (1) are a K^+ penetrating the iron and being identified as a μ^+ , a π^- producing a large shower counter pulse height, or a $\pi + \gamma$ appearing in the same shower counter thus appearing to be an e . Examples of (2) are a μ^+ decay or an e^- from K_{e3} decay. Smaller sources of background are the misidentification of an e in an ee pair as a μ ; or conversely misidentification of a μ in a $\mu\mu$ pair as an e . We have two ways to determine these backgrounds.

A. External Determination

We can determine the background from hadron misidentification or decay by using the three-or-more-prong events of Table I assuming every particle called an e or a μ by the detector was either a misidentified hadron or came from the decay of a hadron. Thus the possibility of anomalous lepton production in 3-or-more prong events is ignored, any such production being included in this background calculation. We use $P_{h \rightarrow a}$ to designate the sum of the probabilities for misidentification or decay causing a hadron h to be called a lepton a . Since the P 's are momentum dependent¹ we use all the eh , μh , and hh events in column 1 of Table II to determine a "hadron" momentum spectrum, and weight the P 's accordingly. For the two data samples we are describing in detail we obtain the momentum averaged probabilities in Table III. Collinear ee

and $\mu\mu$ events are used to determine $P_{e \rightarrow h}$ and $P_{\mu \rightarrow h}$. The statistical errors in the P's in Table III are $\leq 15\%$.

TABLE III

E_{cm} (GeV)	4.8	5.6 to 6.8
$P_{h \rightarrow e}$.18	.19
$P_{h \rightarrow \mu}$.20	.17
$P_{h \rightarrow h}$.62	.64
$P_{e \rightarrow h}$.056	.050
$P_{\mu \rightarrow h}$.08	.08
$P_{e \rightarrow \mu}$.011	.011
$P_{\mu \rightarrow e}$	< .01	< .01

Next we apply the P's in Table III to the column 1 events in Table II. As shown in Table IV, $P_{e \rightarrow \mu}$ or $P_{\mu \rightarrow e}$ are small sources of $e\mu$ background. An additional effect of e misidentification is to send ee events into the eh category; similarly μ misidentification sends $\mu\mu$ events into the μh category, and both misidentifications cause a slight contamination of the hh category. The numbers in these categories corrected for these contaminations and designated by a prime are given in Table IV for use in the next background calculation.

TABLE IV

Summary of background calculations. (The errors in the table are the statistical errors in the determination of the \mathcal{P} 's in quadrature with the statistical error in the number of events.)

E_{cm} (GeV)	4.8	5.6 to 6.8
N_{eh}	20	17
$N'_{\text{eh}} = N_{\text{eh}}$ corrected for ee contamination	15.8	14.8
$N_{\mu\text{h}}$	17	13.5
$N'_{\mu\text{h}} = N_{\mu\text{h}}$ corrected for $\mu\mu$ contamination	14.2	11.2
N_{hh}	14	15
$N'_{\text{hh}} = N_{\text{hh}}$ corrected for ee and $\mu\mu$ contamination	13.8	14.8
$N_{\text{e}\mu}$ background from ee	1.0 ± 0.2	0.5 ± 0.2
$N_{\text{e}\mu}$ background from $\mu\mu$	< 0.4	< 0.3
$N_{\text{e}\mu}$ background from hh calculated using Eq. 3.3	3.7 ± 0.7	3.0 ± 0.6
Total $N_{\text{e}\mu}$ background from sum of preceding 3 rows	4.7 ± 0.7	3.5 ± 0.6
$\tilde{N}_{\text{e}\mu}$ background from hh calculated using only column 1 events and Eq. 3.4	8.1 ± 3.7	5.5 ± 2.6
$N_{\text{e}\mu}$ signature events	24	17

We now come to the major question -- can the $e\mu$ events be due to $P_{h \rightarrow \mu}$ or $P_{h \rightarrow e}$? First a rough calculation using the 4.8 GeV data. Let us suppose that all $e\mu$, eh , μh , and hh events (after correction for $P_{e \rightarrow h}$ and $P_{\mu \rightarrow h}$) are actually hh events. Then for the 4.8 GeV data.

$$N_{hh, \text{true, approximate}} = 67.8 ; \quad (3.1)$$

and the predicted $e\mu$ background is

$$N_{e\mu \text{ background}} = 2 P_{h \rightarrow \mu} P_{h \rightarrow e} N_{hh, \text{true, approximate}} = 4.9 \quad (3.2)$$

Thus only 4 or 5 of the 24 events can be explained in this way! A more exact calculation which makes no assumption about the $e\mu$ events uses

$$N_{hh, \text{true}} = \frac{N'_{eh} + N'_{\mu h} + N'_{hh}}{P_{h \rightarrow h} (P_{h \rightarrow h} + 2 P_{h \rightarrow e} + 2 P_{h \rightarrow \mu})} \quad (3.3)$$

$$N_{e\mu \text{ background from hh}} = 2 P_{h \rightarrow \mu} P_{h \rightarrow e} N_{hh, \text{true}}$$

This leads to the backgrounds listed in Table IV. For both samples the $e\mu$ signal is considerably above the total background calculation.

B. Internal Determination

An important question is whether the 3-or-more prong events are representative of the 2-prong events in Table II. For example, perhaps the K/π ratio is higher in the 2-prong events, or perhaps there is more contamination from the accidental coincidence of a γ and a π in the same shower counter. We have a number of points to make with respect to this question.

- (1) We can calculate $N_{e\mu, \text{background}}$ using just Column 1 events in Table II. Assuming all eh and μh events (after correcting for $P_{e \rightarrow h}$ and $P_{\mu \rightarrow \mu}$ as in Table IV) are misidentified hh events, we use

$$\tilde{N}_{e\mu \text{ background from hh}} = \frac{N'_{eh} N'_{\mu h}}{2N'_{hh}} \quad (3.4)$$

to obtain the $\tilde{N}_{e\mu}$ background from hh in Table IV. This calculation argues against the possibility that the hadronic events in column 1 of Table II are vastly different in character from those in the other columns of Table II or from those in the 3-or-more prong events.

- (2) The $e\mu$ background calculations of Sec. 3A fit within statistics to the number of $e\mu$ events in columns 2 or 3 of Table II.
- (3) Our $P_{e \rightarrow \mu}$ values cannot be too low. If $P_{e \rightarrow \mu}$ were large $N_{e\mu}$ would not decrease while N_{ee} increases as we go from column 1 to column 2.
- (4) The charge distributions of the $e\mu$ events are randomly distributed.
- (5) The isolation of the signature $e\mu$ events depends upon the use of the number of detected photons. It might be argued that the number of photons associated with an event is randomly distributed; and that the large number of $e\mu$ events with 0 photons is just a fluctuation. Table V presents an argument against this for the 4.8 GeV data. If the number of photons is randomly distributed we expect

$$\frac{(46)(40)}{189} = 9.7 \pm 2.2$$

$e\mu$ events with 0 photons, not 24!

TABLE V

Number of photons	0	≥ 1	0 or ≥ 1
$e\mu$	24	16	40
$eh + \mu h + hh$	46	143	189

C. Quality of $e\mu$ Events

Another way to examine the $e\mu$ events is to inquire as to whether the e's and μ 's display all the characteristics expected of such particles. The e's in the $e\mu$ events are selected solely on the basis of large shower counter pulse height. However, they show three additional characteristics of real electrons.

- (1) About 85% of the e's are moving toward muon detection chambers, yet none of them show a signal in these chambers. Hence the e's are not caused by μ misidentification.
- (2) The longitudinal position of an e in a shower counter can be determined by the projection of the particle track, or by the relative pulse heights in the photomultiplier tubes at each end of the shower counter. These two determinations agree within measurement errors. Hence, except possibly for a few events, the e's are not $\pi + \gamma$, $K + \gamma$, or $\mu + \gamma$ combinations in a single shower counter.
- (3) The shower pulse height distribution of the e's in the $e\mu$ events is that of real electrons.

We do not have any tests of the μ quality in the $e\mu$ events which are completely independent of their selection method. However, their shower counter pulse height distribution, and their multiple scattering distributions in passing through the absorbing material are those expected of muons.

D. Background Summary

In the energy range $3.8 \leq E_{cm} \leq 7.8$ GeV we have found

86 $e\mu$ events

The background calculation of Sec. 3A predicts

$$22 \pm 5 \text{ background events ,}$$

and the calculation of Sec. 3B1 predicts

$$30 \pm 6 \text{ background events .}$$

in that sample.

4. EVIDENCE USING IMPROVED MUON DETECTION

In January 1975 an improved muon-pion separation system¹⁵, called the "muon tower", was placed on top of the magnetic detector, Fig. 2. While the primary purpose of this tower was to search for events of the form¹⁵

$$e^+ + e^- \rightarrow \mu + \text{anything} ; \quad (4.1)$$

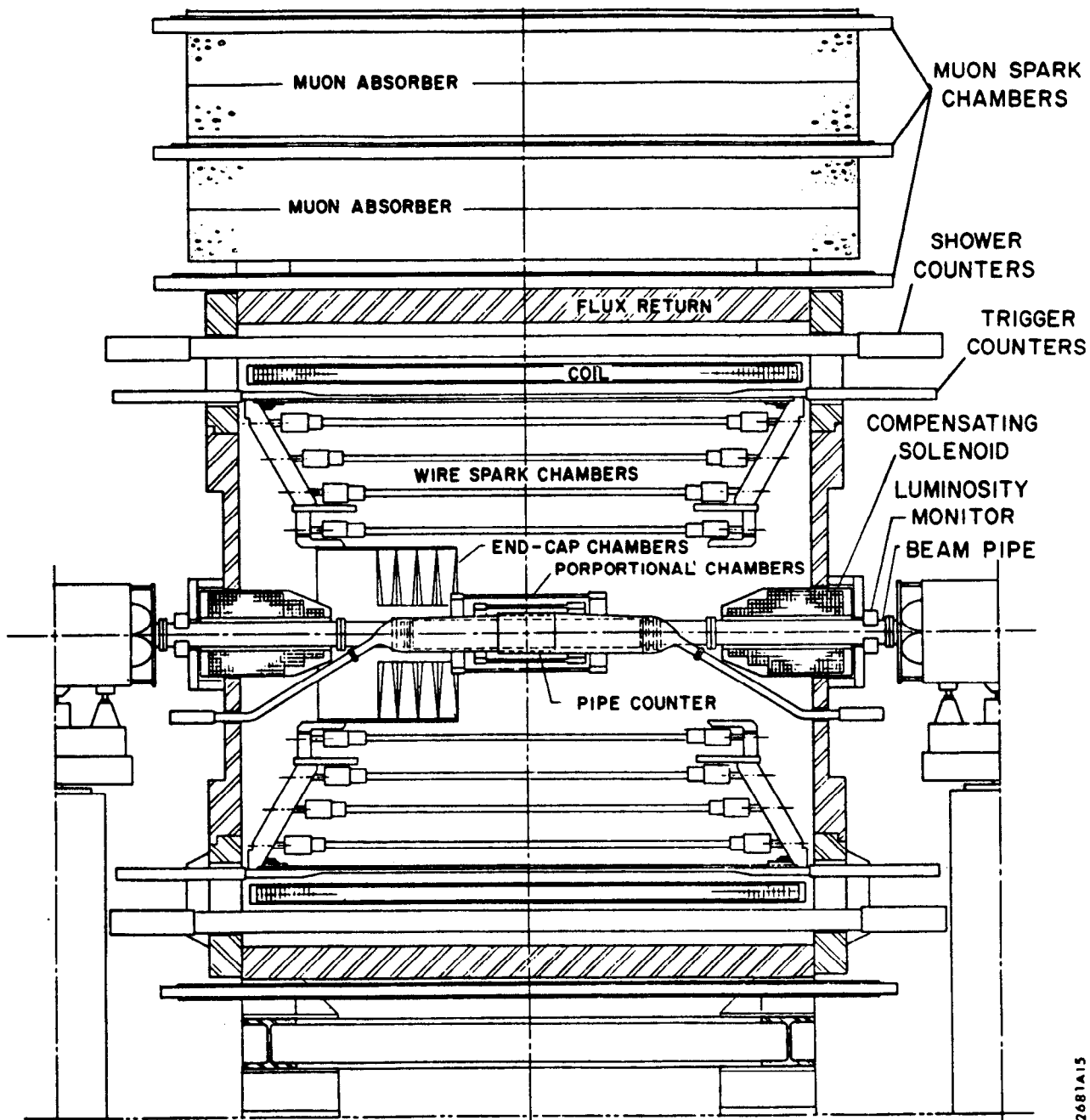
the tower was also used to study the $e\mu$ events. Since the tower only subtends about 15% of the solid angle subtended by the entire detector most $e\mu$ events do not have their μ 's headed toward the tower. Nevertheless the following evidence for $e\mu$ events was found.¹⁵

A muon must have a momentum greater than 0.85 GeV/c to reach the spark chambers between the two muon absorbers (called level 2), and greater than 1.2 GeV/c to reach the topmost spark chambers (called level 3). We then define a muon to be a particle whose track reaches at least to level 2. $P_{h \rightarrow \mu}$, the probability of a hadron appearing to be a muon because of "punch-through" or decay, is now 0.07, rather than about 0.20 as in Sec. 3. Muons so selected we identify by $\underline{\mu}$.

We select all 2-prong events fitting the following criteria. Criteria a, b, and c are the same used to select column 1 events in Table II

(a) Exactly 2 charged tracks with total charge zero visible in the detector.

(b) No photons detected.



2681A15

Fig. 2 Improved muon-pion separation system on magnetic detector.

- (c) $\theta_{\text{copl}} > 20^\circ$.
- (d) One particle headed toward the muon tower with enough momentum to reach level 2.
- (e) The other particle has a momentum of at least 0.65 GeV/c as in Sec. 3.
- (f) The square of the missing mass recoiling against the two particles must be greater than 1.5 (GeV/c)^2 . We use this criterion to eliminate $\mu\gamma$ events and simplify the analysis. During part of the data-taking there were no muon detection chambers diametrically opposite the tower.

Using these criteria we found.¹⁵

$$\begin{aligned}
 &10 \text{ ee events} \\
 &5 \text{ } e\bar{\mu} \text{ events} \\
 &10 \text{ } \mu\bar{\mu} \text{ events} \\
 &32 \text{ events with other particle combinations}
 \end{aligned}
 \tag{4.1}$$

The major source of background¹⁵ is the 32 events, assuming they are all hh (hadron-hadron) pairs. Taking even the 5 $e\bar{\mu}$ events as hh pairs we calculate

$$\begin{aligned}
 N_{e\bar{\mu} \text{ background}} &= P_{h \rightarrow e} P_{h \rightarrow \mu} \quad (37) \\
 &= (.20)(.07)(37) = 0.52
 \end{aligned}$$

Hence only 0.52 of the 5 $e\bar{\mu}$ events can be explained by conventional means.

5. GENERAL PROPERTIES AND OBSERVED CROSS SECTIONS

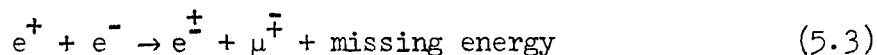
I have already implied by Eq. 1.1 that the $e\mu$ events consists of $e + \mu + \geq 2$ undetected particles. Letting p_e, p_μ, p_i be respectively the four-momentum of the e , and μ and of the entire initial state; we define the invariant mass squared

$$M_i^2 = (p_e + p_\mu)^2 ; \quad (5.1)$$

and the missing mass squared

$$M_m^2 = (p_i - (p_e + p_\mu))^2 . \quad (5.2)$$

The distributions in M_i^2 and M_m^2 are shown in Fig. 3 for the $E_{cm} = 4.8$ GeV data; the σ of M_m^2 is roughly 0.6 GeV^2 . This distribution means that in the reaction



at least two particles are not detected. Data at all other energies shows the same phenomena, with the upper limit of the M_m^2 distribution increasing as E_{cm} increases.

Figure 4 shows the observed cross section in the detector acceptance for signature $e\mu$ events versus center-of-mass energy with the background subtracted at each energy as described in Sec. 3. There are a total of 86 $e\mu$ events summed over all energies, with a calculated background of 22 events or 30 events as discussed in Sec. 3. The corrections to obtain the true cross section for the angle and momentum cuts used here depend on the hypothesis as to the origin of these $e\mu$ events and the corrected cross section can be many times larger than the observed cross section. While Fig. 4 shows an apparent threshold at around 4 GeV, the statistics are small and the correction factors are largest for low \sqrt{s} . This is discussed further in Sec. 8.

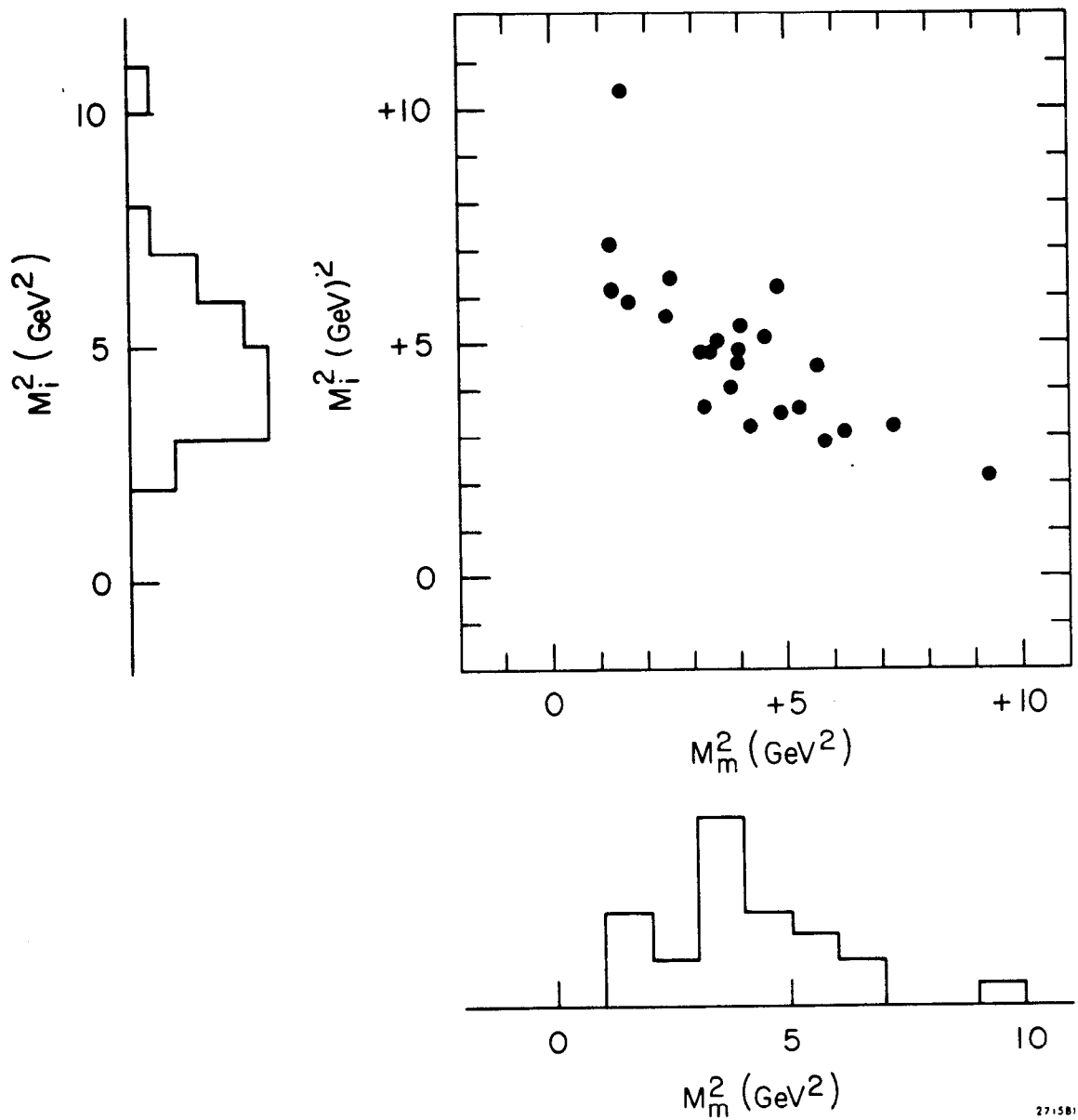


Fig. 3 Distribution of M_1^2 versus M_m^2 for the $E_{cm} = 4.8$ GeV signature $e\mu$ events.

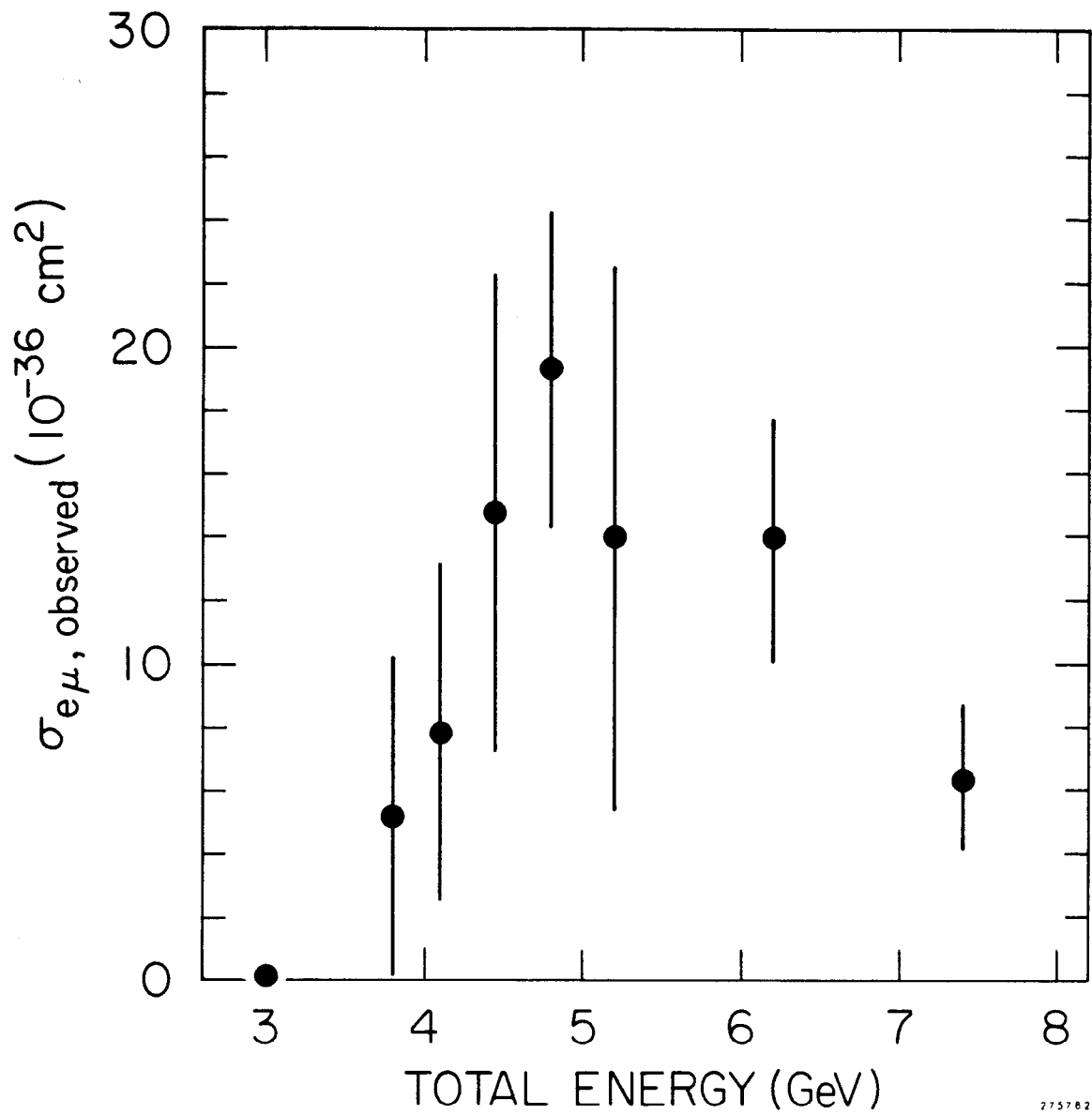


Fig. 4 The observed cross section for the $e\mu$ events.

In Fig. 5 we show the background cross section which was subtracted¹⁶ from the signature $e\mu$ event cross section to give $\sigma_{e\mu, \text{observed}}$ in Fig. 4.

6. ANGULAR DISTRIBUTIONS

We define the collinearity angle by

$$\cos \theta_{\text{coll}} = -\vec{p}_e \cdot \vec{p}_\mu / (|\vec{p}_e| |\vec{p}_\mu|) \quad (6.1)$$

When the e and μ are moving in exactly opposite directions $\theta_{\text{coll}} = 0$. The $\cos \theta_{\text{coll}}$ distribution is shown in Fig. 6. (There is no background subtraction here.) The small angle behavior of the θ_{coll} distribution is due to the $\theta_{\text{coll}} < 20^\circ$ cut. All $\theta_{\text{coll}} < 20^\circ$ are eliminated and larger θ_{coll} are partially lost. At the higher E_{cm} energies the $\cos \theta_{\text{coll}}$ distribution is naturally fit by the hypothesis

$$\begin{aligned} e^+ + e^- &\rightarrow U^+ + U^- , \\ U &\rightarrow e + X , \mu + X , \end{aligned} \quad (6.2)$$

where X represents one or more neutral particles; when $|\vec{p}_e| > 0.65 \text{ GeV}/c$, $|\vec{p}_\mu| > 0.65 \text{ GeV}/c$ are taken into account.

At the lower energies the nature of X becomes important. We consider two possibilities for the decay of the U

$$\begin{aligned} \text{2-body decay : } U^- &\rightarrow e^- + \bar{\nu}_e \quad \text{and} \quad (6.3) \\ &U^- \rightarrow \mu^- + \bar{\nu}_\mu \end{aligned}$$

$$\begin{aligned} \text{3-body decay : } U^- &\rightarrow \nu_U + e^- + \bar{\nu}_e \quad \text{and} \quad (6.4) \\ &U^- \rightarrow \nu_U + \mu^- + \bar{\nu}_\mu \end{aligned}$$

The 2-body decay could be from a meson or elementary boson. The 3-body decay could be from a heavy lepton. For convenience I shall assume the mass of the ν_U is zero and the $U-\nu_U$ current is V-A. (I will not consider the effect of a V + A current or of the mass of the ν_U being non-zero.)

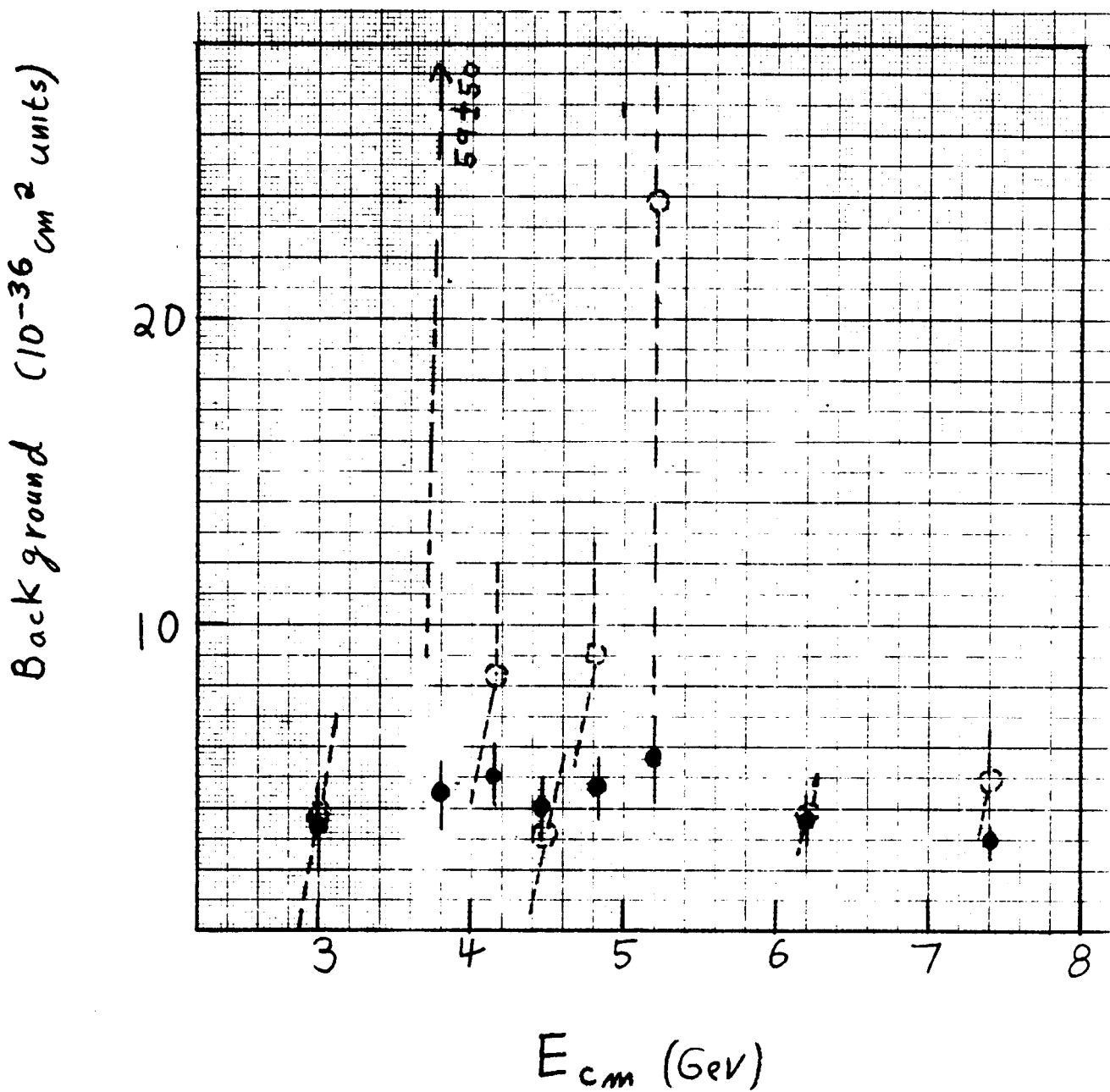


Fig. 5 The solid circles are the background calculated according to the method of Sec. 3A. This background was subtracted from the data to yield the observed cross section in Fig. 4. The dashed circles are the background calculated using only column 1 events from Table II according to the method described in Sec. 3B1 and Eq. 3.4. The statistical errors are much larger with this method. On the average the second method yields about 50% more background events than the first method.

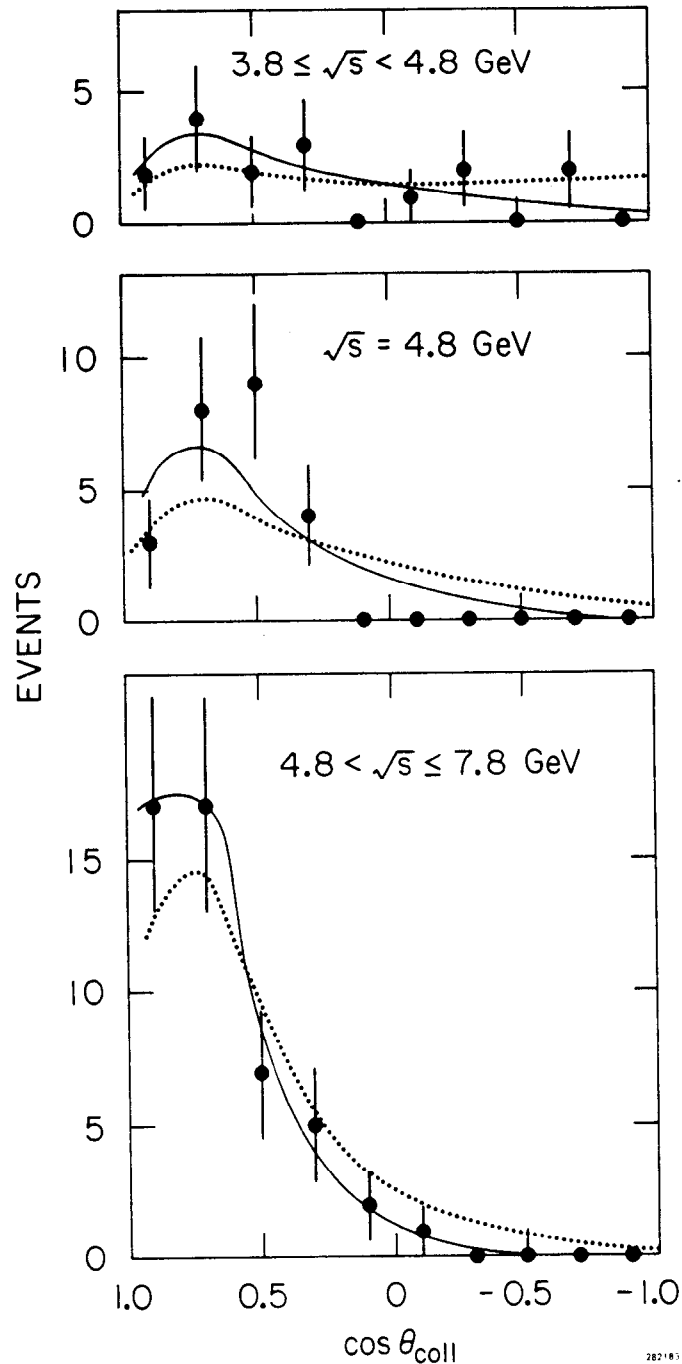
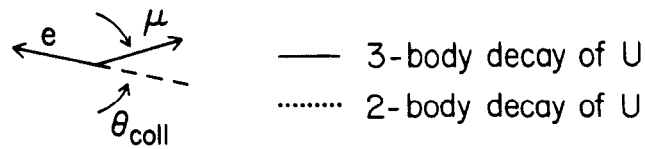


Fig. 6 The distribution in $\cos \theta_{\text{coll}}$ for three different $\sqrt{s} = E_{\text{cm}}$ intervals. The solid curve is for the production of a pair of U particles, the U taken to be a heavy lepton of $1.8 \text{ GeV}/c^2$ mass coupled to its massless neutrino through V-A. Hence each U undergoes the 3-body decay of Eq. 6.4 in the text. The dotted curve is for the production of a pair of U particles, the U taken to be a boson of $1.9 \text{ GeV}/c^2$ mass decaying through its purely leptonic decay mode. Hence each U undergoes the 2-body decay of Eq. 6.3 in the text. In the calculation of both curves all spin-spin correlations are ignored.

Also I will not discuss here semi-leptonic decays of a meson, baryon, or boson.) All spin-spin correlations are ignored.

Using the hypotheses in Eqs. 6.3 and 6.4 and the θ_{coll} distributions we can determine a rough upper limit on the U mass (M_U). The simple rule is that at fixed E_{cm} , as M_U increases the probability of obtaining large θ_{coll} values increases. Table VI shows some examples (These numbers are calculated for the 0.65 GeV/c momentum cuts on the e and μ).

TABLE VI

Comparison of the number of $\theta_{\text{coll}} > 90^\circ$ $e\mu$ events (penultimate row) with various U masses and U decay hypotheses. (Note that the last row gives the total number of $e\mu$ events for use in statistical tests.)

E_{cm} (GeV)		Number $e\mu$ events with $\theta_{\text{coll}} > 90^\circ$		
		3.8 to 4.8	4.8	4.8 to 7.8
Decay Mode	Mass (GeV/c ²)			
3-body V-A (Eq. 6.4)	1.6	1.4	0.8	0.3
	1.8	4.0	2.7	1.3
	2.0	5.2	6.0	2.9
	2.2		10.7	7.0
2-body (Eq. 6.3)	1.6	2.8	2.1	0.9
	1.8	6.0	4.7	2.8
	2.0	6.1	8.8	5.8
	2.2		12.2	10.1
Data $e\mu$ events with $\theta_{\text{coll}} > 90^\circ$		5	0	1
Data <u>total</u> number of $e\mu$ events		16	24	49

We see that masses much greater than $2.0 \text{ GeV}/c^2$ cannot fit the θ_{coll} distribution, using the hypothesis of Eqs. 6.3 or 6.4. We could go to higher masses in the 3-body decay case if we use $V + A$ or set the mass of the ν_U to be non-zero. In this paper I shall show fits to the data using $M_U = 1.9 \text{ GeV}/c$ for the 2-body decay and $M_U = 1.8 \text{ GeV}/c^2$ for the 3-body decay. These masses are examples which seem to fit the angle and momentum distributions. But masses in the range of 1.6 to $2.0 \text{ GeV}/c^2$ are acceptable, and with special assumptions one might go up to $2.2 \text{ GeV}/c^2$.

Returning to Fig. 6, particularly in the 4.8 GeV data the 2-body hypothesis has difficulty in explaining the small number of large θ_{coll} events. Reduction of M_U can cure this, but then problems arise, Sec. 7, with the momentum distribution of the e and μ . An alternative cure requires strong spin-spin correlation between the mesons.² A 3-body decay mode obviously fits the $\cos \theta_{\text{coll}}$ distributions in a more natural manner. However, a mixture of two mechanisms -- one U pair with a 3-body decay mode and the other U pair with a 2-body decay mode -- will obviously fit the data.

Returning to background questions, Fig. 7 shows the $\cos \theta_{\text{coll}}$ distributions for 2-prong, zero photon, hadron-hadron events -- the events which when misidentified as $e\mu$'s are the major contamination. We note that the $\cos \theta_{\text{coll}}$ distribution is peaked at small θ_{coll} as in the $e\mu$ events. Hence the background in the $e\mu$ events cannot be separated out by using θ_{coll} . However we note that as E_{cm} increases the $\cos \theta_{\text{coll}}$ distribution for the $e\mu$ events becomes increasingly peaked forward while the distribution for the hadron-hadron events remains roughly the same.

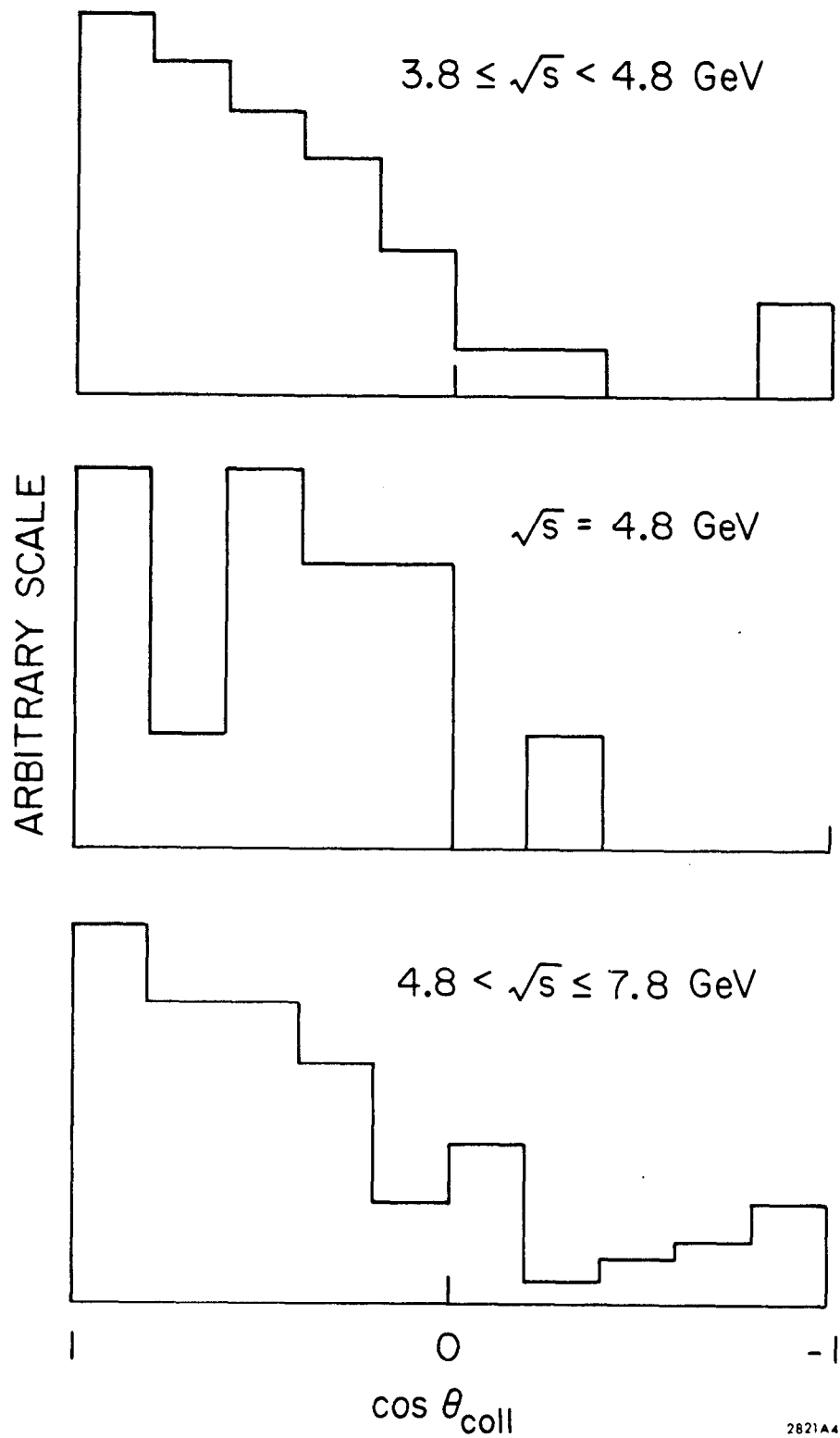


Fig. 7 $\cos \theta_{\text{coll}}$ distribution for 2-prong, zero photon, hadron-hadron events.

7. MOMENTUM DISTRIBUTIONS

Figures 8 and 9 show the momentum distributions of the e and μ in the $e\mu$ events. In Fig. 9 the kinematic limits on p_e and p_μ for various M_U are given. (The μ mass is set to zero.) This limit is the same for the 2-body and 3-body decay modes providing the neutral particle masses are all zero -- and this is indeed what is assumed. We note that unless we are willing to attribute some data points to background, M_U must be of the order of $2 \text{ GeV}/c^2$ or less. To combine the data from different E_{cm} runs we show in Figs. 10 and 11 the distributions in

$$\rho = \frac{p - 0.65}{p_{\text{max}} - 0.65} \quad , \quad p \text{ in GeV}/c \quad ; \quad (7.1)$$

where p_{max} is calculated for $M_U = 1.8 \text{ GeV}$ (the use of $M_U = 1.9$ makes very little difference) and p is $|p_e|$ or $|p_\mu|$. Each event thus appears twice. Figures 10 and 11 are corrected for background.

The solid and dotted curves in Figs. 10 and 11 are the predicted distributions for the 3-body and 2-body decay modes of the U respectively (Eqs. 6.4 and 6.3). All spin-spin correlations are ignored in these calculations. The bump at the high ρ end of the dotted curves occurs because of the events at $E_{\text{cm}} = 3.8 \text{ GeV}$ -- the threshold for $M_U = 1.9$ particles. Incidentally if we distort the predicted 2-body decay mode θ_{coll} distribution to fit the σ_{coll} distribution data, we obtain the dashed curves in Figs. 10 and 11. Thus we see that the 2-body decay mode usually predicts too many large ρ , that is large p , points. Only at 4.8 GeV are the 2-body and 3-body hypotheses equally applicable.

8. DISCUSSION AND CONCLUSIONS

Our studies of the reaction



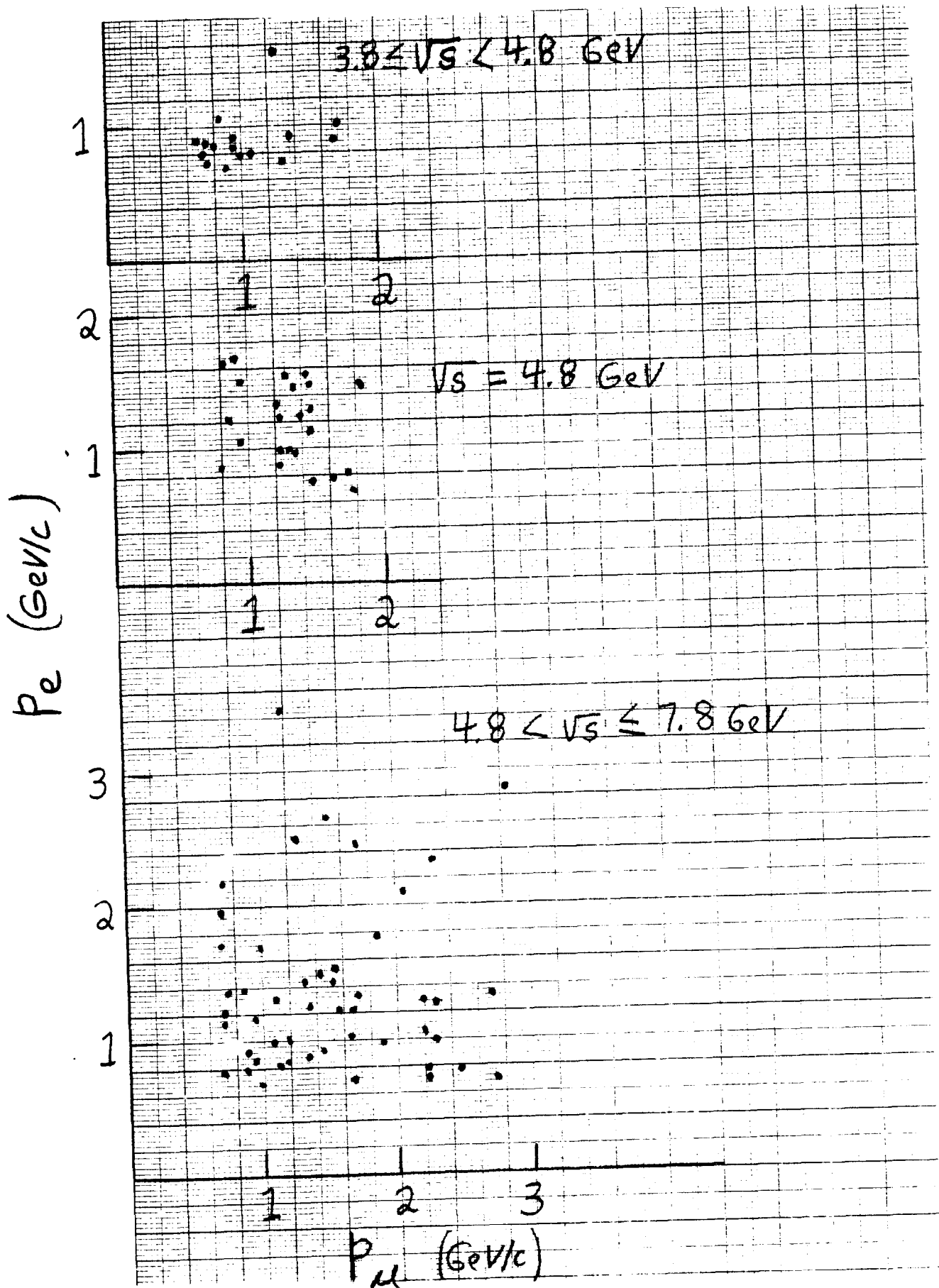


Fig. 8 The distribution of P_e versus P_μ for the $e\mu$ events in different $E_{cm} = \sqrt{s}$ intervals.

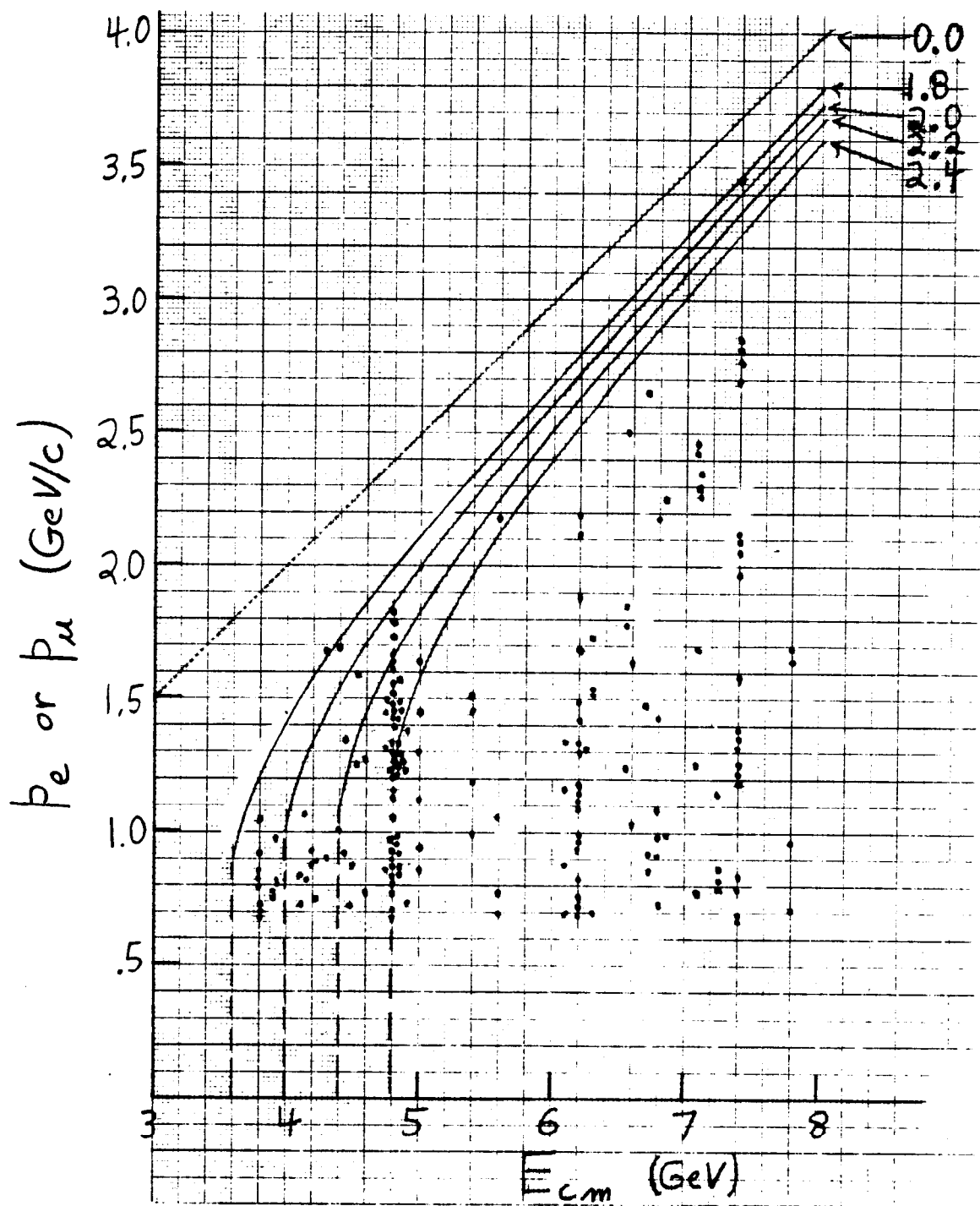


Fig. 9 Distribution of p_e and p_μ for all $e\mu$ events. The curves are upper limits on p_e or p_μ for the indicated U masses in GeV/c^2 . These limits are the same for 2-body and 3-body decay provided all neutral masses are zero.

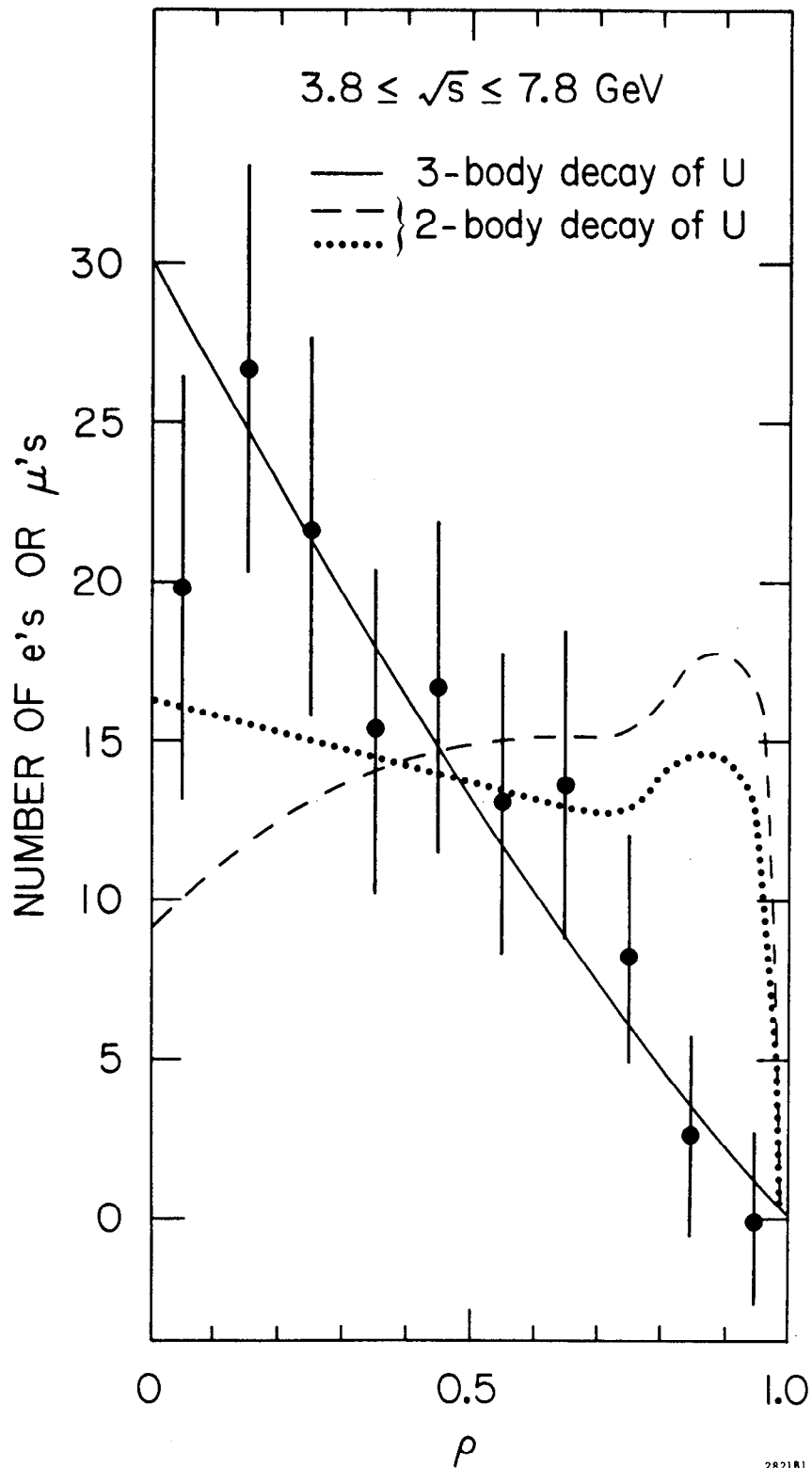


Fig. 10 The distribution in $\rho = (p - 0.65)/(p_{\max} - 0.65)$ (p in GeV/c) for all \sqrt{s} . The solid and dotted curves are defined in the caption to Fig. 6. The dashed curve is the same as the dotted curve except that the θ_{coll} distribution has been distorted to fit the data in Fig. 6.

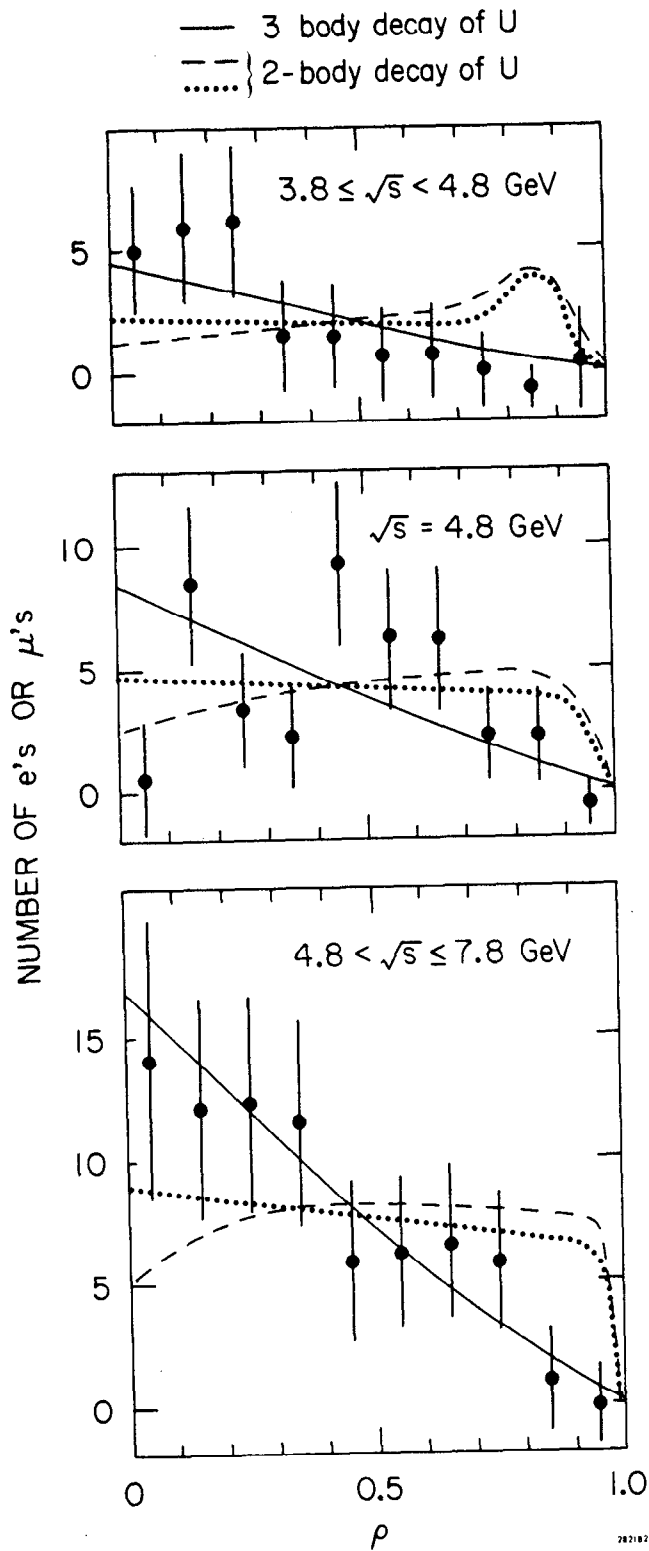


Fig. 11 The distribution in ρ for three intervals in \sqrt{s} . See caption to Figs. 6 and 10 for meaning of curves.

are not complete by any means. However we can draw some conclusions.

- (1) We believe that anomalous $e\mu$ events described by Eq. 8.1 exist because we have not yet found any conventional explanation for all such events. Only 20 to 35% of them can be explained by various background mechanisms.
- (2) The data are consistent with the hypothesis of the production of pairs of new particles of one or more types $U_1, U_2 \dots$

$$\begin{aligned}
 e^+ + e^- &\rightarrow U_1^+ + U_1^- \\
 e^+ + e^- &\rightarrow U_2^+ + U_2^- \\
 &\dots \dots \dots
 \end{aligned}
 \tag{8.2}$$

provided at least one of these types has 3-body decay modes.

- (3) The data is not consistent with all the events coming from 2-body leptonic decays of the U's.
- (4) We know of nothing which is inconsistent with the hypothesis that all the events come from the 3-body decay of a U particle. In particular the 3-body decay could be the purely leptonic decay of a sequential heavy lepton.
- (5) The observed production cross section does not determine the nature of the U. In Fig. 12 $\sigma_{e\mu, \text{observed}}$ is fitted with three different hypotheses:
 - (a) The U is a sequential heavy lepton ℓ of mass $1.8 \text{ GeV}/c^2$ with V-A coupling and a massless neutrino. The production cross section is given by Eq. 1.8.

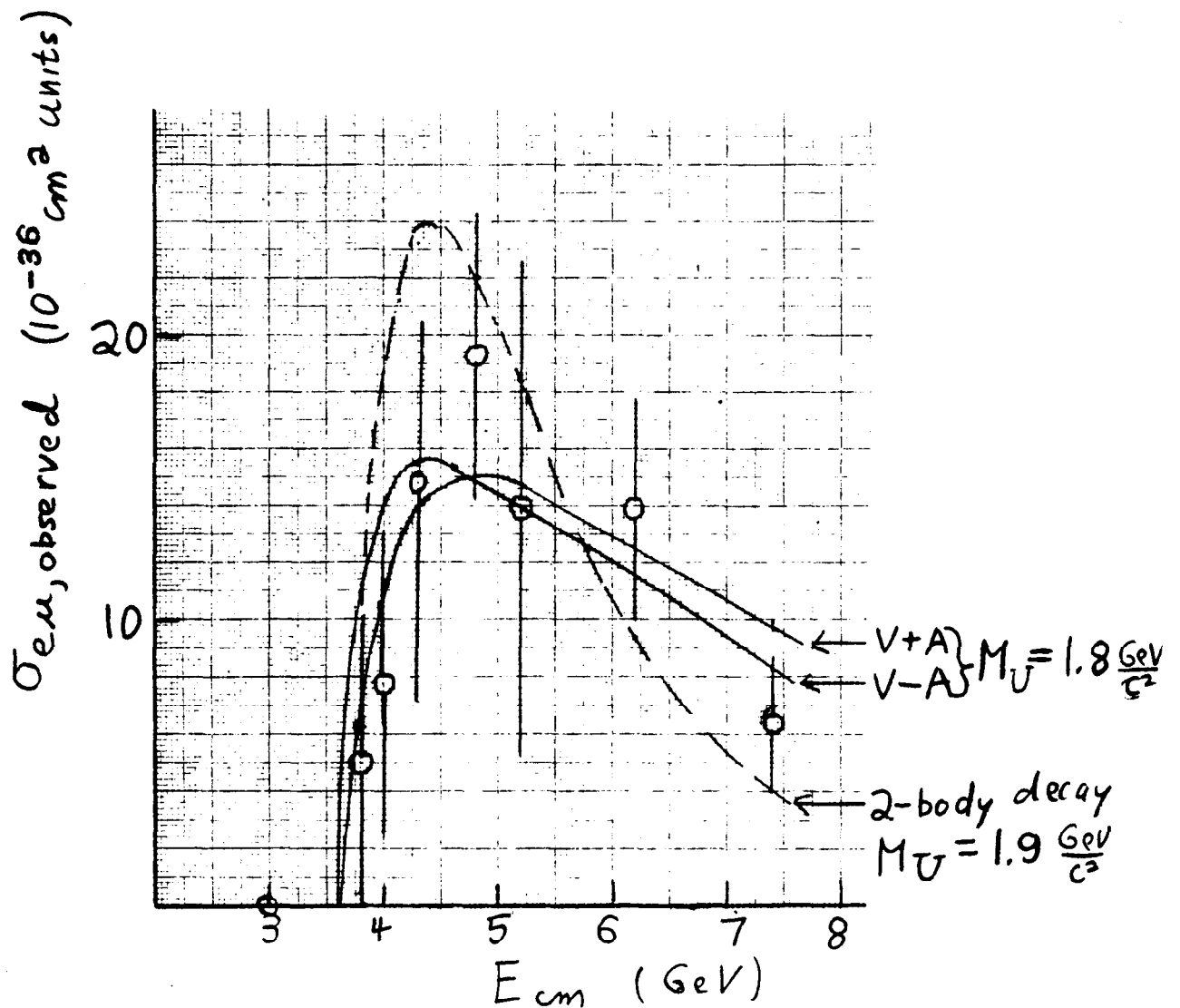


Fig. 12 Fits to $\sigma_{e\mu}$, observed. The solid curves are for the production of a pair of $1.8 \text{ GeV}/c^2$ mass leptons (U) assuming purely leptonic decay with V+A or V-A for the $U - \gamma_U$ current as indicated. The dashed curve is for the production of a pair of $1.9 \text{ GeV}/c^2$ mass bosons (U) assuming 2-body, purely leptonic decay modes, a production form factor $F = \text{constant}/s$, and a production cross section given by Eq. 8.5. All neutrinos are massless.

(b) The U is a sequential heavy lepton ℓ of mass $1.8 \text{ GeV}/c^2$ with V+A coupling and a massless neutrino. The production cross section is given by Eq. 1.8.

(c) The U is a meson M of mass $1.9 \text{ GeV}/c^2$ with the 2-body decay of Eq. 6.3. The production cross section is given by Eq. 1.11 with

$$F(s) = \text{constant}/s ; \quad (8.3)$$

a form factor that decreases rapidly with increasing E_{cm} .

As shown in Table VII all three hypotheses are reasonable fits to the data.¹⁷ Also shown in Table VII are the leptonic branching ratios for the heavy lepton assuming

$$R_{\text{leptonic}} = \frac{\Gamma(\ell^- \rightarrow \nu_\ell + e^- + \bar{\nu}_e)}{\Gamma(\ell^- \rightarrow \text{all modes})} = \frac{\Gamma(\ell^- \rightarrow \nu_\ell + \mu^- + \bar{\nu}_\mu)}{\Gamma(\ell^- \rightarrow \text{all modes})} \quad (8.4)$$

Such ratios are compatible with conventional theories of heavy lepton decay.^{3,5} For the meson hypotheses we do not know the production cross section theoretically, hence we cannot calculate a unique R_{leptonic} . For comparison purposes I arbitrarily combine the constants in Eqs. 1.11 and 8.3 to give

$$\sigma_{ee \rightarrow MM} = \frac{4\pi \alpha^2 \beta^3}{3s} \left(\frac{4 m_M^2}{s} \right)^2 \quad (8.5)$$

compared to

$$\sigma_{ee \rightarrow \ell\ell} = \frac{4\pi \alpha^2 \beta}{3s} \left[\frac{3 - \beta^2}{2} \right] \quad (8.6)$$

Here m_M is the mass of the meson M.

The

$$R_{\text{leptonic}} = \frac{\Gamma(M^- \rightarrow e^- + \bar{\nu}_e)}{\Gamma(M^- \rightarrow \text{all modes})} = \frac{\Gamma(M^- \rightarrow \mu^- + \bar{\nu}_\mu)}{\Gamma(M^- \rightarrow \text{all modes})} \quad (8.7)$$

in Table VII is for Eq. 8.5.

TABLE VII

	χ^2 for 6 degrees of freedom	R_{leptonic}
3-body, V-A $M_\rho = 1.8 \text{ GeV}/c^2$	4.3	0.17
3-body, V+A $M_\rho = 1.8 \text{ GeV}/c^2$	3.8	0.17
2-body, $M_M = 1.9 \text{ GeV}/c^2$ σ_{prod} given in Eq. 8.5	9.8	0.36 see text

We still have to answer the following questions

- (1) It is very unlikely that semi-leptonic decays account for all the events. For example, a semi-leptonic decay mode of a new meson (Eq. 1.10) of the form

$$M^- \rightarrow e^- + \bar{\nu}_e + K_L^0, \quad M^- \rightarrow \mu^- + \bar{\nu}_\mu + K_L^0 \quad (8.8)$$

cannot account for all the $e\mu$ events, because we do not see a substantial signal with 2 π 's from

$$M^- \rightarrow e^- + \bar{\nu}_e + K_S^0 \quad \text{or} \quad M^- \rightarrow \mu^- + \bar{\nu}_\mu + K_S^0 \quad (8.9)$$

in multiprong data. However we have not yet ruled out completely the decay modes in Eqs. 8.9. Questions about these and other semi-leptonic decay possibilities are still being studied.

- (2) We do not yet know if a sequential heavy lepton is completely consistent with all the data. In particular if we do not find hadronic decay modes, the U cannot be a sequential heavy lepton. This is because the observed leptonic decay modes are not sufficiently large to yield the expected production cross section, Eq. 8.6.
- (3) We do not know if there is any other single hypothesis consistent with the data.
- (4) Finally we do not know if more than one thing is going on. That is, are there several mechanisms producing $e\mu$ events -- both new mesons and new leptons or several sets of new mesons, for example?

9. ACKNOWLEDGEMENTS

This data is the work of the SLAC-LBL Magnetic Detector Collaboration¹ and hence many individuals have contributed in crucial ways to the results presented here in this summary talk.

REFERENCES

1. M.L. Perl et al., SIAC-PUB-1626 (submitted to Phys. Rev. Letters).
2. M.L. Perl, SIAC-PUB-1592 (to be published in Proceedings of the Canadian Institute of Particle Physics Summer School, McGill University, 1975).
3. A review as of October, 1974 on heavy lepton theories and searches is M.L. Perl and P. Rapidis, SIAC-PUB-1496 (1974) (unpublished).
4. J.D. Bjorken and C.H. Llewellyn Smith, Phys. Rev. D7, 88 (1973).
5. Y.S. Tsai, Phys. Rev. D4, 2821 (1971).
6. K. Fujikawa and N. Kawamoto, Institute for Nuclear Study Report INS-Rep-239 (1975).
7. For examples see A. De Rujula et al., Phys. Rev. Lett. 35, 628 (1975); T.C. Yang, Univ. of Maryland Preprint (unnumbered, 1975).

8. M.K. Gaillard, B.W. Lee, and J.L. Rosner, Rev. Mod. Phys. 47, 277 (1975).
9. M.B. Einhorn and C. Quigg, FERMILAB-PUB-75/21-THY, to be published in Phys. Rev.
10. M. Goldhaber, Phys. Rev. Lett. 1, 1521 (1958).
11. B.C. Barish et al., Phys. Rev. Lett. 31, 233 (1975).
12. J.-E. Augustin et al., Phys. Rev. Lett. 34, 233 (1975).
13. G.J. Feldman and M.L. Perl, Phys. Rept. 19C, 233 (1975).
14. For reviews of this subject see V.M. Budner et al., Phys. Rept. 15C, 182 (1975); H. Terazawa, Rev. Mod. Phys. 46, 615 (1973). We are indebted to S. Brodsky for very useful discussions on this reaction.
15. G.J. Feldman, Proceedings of the 1975 International Symposium on Lepton and Photon Interactions at High Energies (SIAC, 1975).
16. At $E_{\text{cm}} = 3.0$ GeV there were zero $e\mu$ events and $\sigma_{e\mu, \text{observed}}$ was given as zero in Fig. 4, but there is a background cross section at 3.0 GeV as shown in Fig. 5.
17. See also H. Harrari, ibid., where the relation of what Harrari calls "new e^+e^- physics" versus "old e^+e^- physics" is discussed.